MOLECULAR AND CELLULAR BIOLOGY, Jan. 2008, p. 666–677 Vol. 28, No. 2
0270-7306/08/$08.00+0 doi:10.1128/MCB.01716-07

GRP78 and Cripto Form a Complex at the Cell Surface and Collaborate To Inhibit Transforming Growth Factor β Signaling and Enhance Cell Growth[▽]

Gidi Shani, Wolfgang H. Fischer, Nicholas J. Justice, Jonathan A. Kelber, Wylie Vale, and Peter C. Gray*

Clayton Foundation Laboratories for Peptide Biology, The Salk Institute for Biological Studies, La Jolla, California 92037

Received 18 September 2007/Accepted 26 October 2007

Cripto is a multifunctional cell surface protein with important roles in vertebrate embryogenesis and the progression of human tumors. While Cripto has been shown to modulate multiple signaling pathways, its binding partners do not appear to fully explain its molecular actions. Therefore, we conducted a screen aimed at identifying novel Cripto-interacting proteins. This screen led to our identification of glucose-regulated protein 78 (GRP78), an endoplasmic reticulum (ER) chaperone that is also expressed at the surfaces of tumor cells. Here we demonstrate that Cripto and GRP78 interact at the cell surfaces of multiple cell lines and that their interaction is independent of prior association within the ER. Interestingly, short hairpin RNA knockdown of endogenous GRP78 resulted in enhanced transforming growth factor β (TGF-β) signaling, indicating that like Cripto, GRP78 inhibits this pathway. We further show that when coexpressed, GRP78 and Cripto collaborate to antagonize TGF-β responses, including Smad phosphorylation and growth inhibition of prostate cancer cells grown under anchorage-dependent or -independent conditions. Finally, we provide evidence that cells coexpressing GRP78 and Cripto grow much more rapidly in soft agar than do cells expressing either protein individually. Together, our results indicate that these proteins bind at the cell surface to enhance tumor growth via the inhibition of TGF-β signaling.

Cripto (Cripto-1, teratocarcinoma-derived growth factor 1) is a small, glycosylphosphatidylinositol-anchored signaling protein with essential physiological roles during embryogenesis. The protein is also expressed at high levels in human tumors and has been linked to several aspects of tumor initiation and progression, including increased cellular proliferation, migration, invasion, tumor angiogenesis, and epithelial-to-mesenchymal transition (34).

Multiple mechanisms of action have been attributed to Cripto that are thought to underlie its oncogenic function (34). For example, it modulates the signaling of transforming growth factor β (TGF-β) superfamily members by forming complexes with some of these ligands and their respective signaling receptors. In this context, Cripto has an obligatory role in facilitating signaling by certain ligands, such as Nodal (29, 30), while inhibiting signaling by activins (1, 12) and TGF-β1 (13). Since activins and TGF-βs have tumor suppressor functions (27), the inhibition of their signaling by Cripto provides a mechanism that may at least partly explain the ability of Cripto to promote tumor growth (1, 12, 13). Conversely, Cripto-dependent Nodal signaling may contribute to late stages of tumor growth and metastasis under conditions in which cells have become refractory to growth-inhibitory effects of TGF-β ligands (27, 35).

Cripto can also be released from the cell in a soluble form and act in a manner resembling that of secreted growth factors (34). In this regard, it was reported that Cripto and the *Xenopus* Cripto ortholog FRL-1 cause the phosphorylation of ErbB-4 (4) and FGFR-1 (16), respectively. Cripto does not bind these proteins directly, however, and a putative Cripto receptor mediating these phosphorylation events has yet to be found (4, 16). In this regard, although Cripto possesses an epidermal growth factor (EGF)-like domain and resembles EGF receptor ligands, it does not directly bind to any members of the EGF receptor family (4). Furthermore, while Cripto binds the extracellular glycosylphosphatidylinositol-anchored proteoglycan glypican-1 to cause activation of mitogen-activated protein kinase and PI3K pathways via c-Src, a transmembrane protein mediating this action has not yet been identified (5).

Therefore, while Cripto has multiple signaling mechanisms that may contribute to tumor growth, its known cell surface binding partners do not appear to fully explain its reported oncogenic functions. In order to identify novel Cripto-interacting proteins, we have conducted a protein interaction screen using full-length, membrane-anchored Cripto as bait. This screen led to the identification of glucose-regulated protein 78 (GRP78), a multifunctional regulator of endoplasmic reticulum (ER) homeostasis that has also been heavily implicated in cancer (19). Interestingly, although generally localized to the ER, GRP78 is also selectively expressed at the plasma membrane in tumor cells and we show here that Cripto binds GRP78 at the cell surface. We provide further evidence that Cripto and GRP78 interact in a cell-free system in a manner that does not require their association within the ER. Finally, we show that GRP78 and Cripto cooperate to attenuate TGF-β-dependent growth-inhibitory effects and increase colony growth of prostate cancer cells in soft agar. Together, our

* Corresponding author. Mailing address: Clayton Foundation Laboratories for Peptide Biology, The Salk Institute, La Jolla, CA, 92037. Phone: (858) 453-4100, ext. 1689. Fax: (858) 552-1546. E-mail: gray@salk.edu.

▽ Published ahead of print on 8 November 2007.

results indicate that these two proteins form a complex at the cell surface and thereby confer a growth advantage to tumor cells via inhibition of TGF-β signaling.

MATERIALS AND METHODS

Materials. NuPAGE gels, molecular weight standards and the CyQUANT cell proliferation assay kit were from Invitrogen (San Diego, CA). Sulfo-NHS-LC-biotin was purchased from Pierce (Rockford, IL). TGF-β1 was purchased from R&D Systems (Minneapolis, MN). Anti-Flag (M2), antihemagglutinin (anti-HA) (HA-7), anti-His (His-1), and anti-pan-cadherin antibodies, as well as anti-Flag M2 gel beads, Flag peptide, and thapsigargin, were purchased from Sigma-Aldrich (St. Louis, MO). Anti-GRP78 (N-20 and 76-E6), anti-TβRII (C16), and protein G-PLUS-agarose beads were from Santa Cruz Biotechnology (Santa Cruz, CA). Anti-GRP78 (KDEL) was from Stressgen Bioreagents (Ann Arbor, MI). Anti-phospho-Smad2, anti-TβRI, and anti-pan-actin were purchased from Cell Signaling (Danvers, MA). The p26-Flag expression construct was a generous gift from Kuo Fen Lee (Peptide Biology Laboratories, Salk Institute). Antibodies directed against Cripto (rabbit 6900) were raised against a peptide spanning mouse Cripto amino acids 81 to 97 and cyclized between Cys 81 and Cys 90. Smad2 antisera were raised against a peptide conserved between Smad2 and Smad3, spanning amino acids 159 to 175 of human Smad3. Polyclonal antisera targeting the Flag epitope (rabbit 6643) were raised against a 2× Flag peptide. Rabbit polyclonal anti-Cripto, anti-Smad2/Smad3, and anti-Flag antisera were produced by Joan Vaughan (Peptide Biology Laboratories, Salk Institute).

Expression constructs, cell lines, and transient transfection. The wild-type and mutant mouse Cripto-Flag expression constructs have previously been described (13). Cripto constructs were also generated in the lentiviral vector pCSC (26) for the production of lentivirus. Lentiviral vectors used in this study were a generous gift from Inder Verma (Salk Institute). The TβRI-HA and TβRII-His expression constructs were gifts from Joan Massagué (Memorial Sloan-Kettering Cancer Center, New York, NY). Standard PCR techniques were used to generate the human GRP78 construct with an HA epitope at its C terminus. 293T cells, P19 cells, and HeLa cells were grown in Dulbecco's modified Eagle's medium, and PC3 cells were grown in F-K12 medium. Media were supplemented with 10% fetal calf serum (293T, HeLa, and PC3) or 7.5% fetal calf serum (P19), together with penicillin, streptomycin, and L-glutamine. For transient transfection, 293T cells were plated on polylysine-coated, 15-cm plates ($\sim 10^7$ cells/plate) and then transfected the following day at about 40 to 60% confluence using the polyethyleneimine transfection reagent as previously described (14).

Mass spectrometric analysis. Mass-specific bands were excised from a Coomassie blue-stained gel. Gel slices were further destained by treatment with 40% aqueous *n*-propanol and 50% aqueous acetonitrile. To the destained gel slice, 100 ng trypsin was added in 10 μl ammonium bicarbonate solution (20 mM). Digestion was allowed to proceed at 37°C for 16 h. One microliter of the supernatant was spotted onto a matrix-assisted laser desorption ionization target and mixed with 1 μl of a saturated solution of alpha-cyano-hydroxycinnamic acid. After being dried, the sample was analyzed on a Bruker Ultraflex TOF/TOF (Bruker Daltonics, Billerica, MA) instrument in positive reflected time-of-flight (TOF) mode. Mass fingerprint data were analyzed using the Mascot algorithm (Matrix Science, London, United Kingdom).

Fluorescence imaging. 293T cells (35,000 per well) and P19 cells (500,000 per well) were plated in 12-well plates and grown overnight on coverslips pretreated with polylysine. Cells were washed with potassium-phosphate-buffered saline (KPBS), fixed in 4% paraformaldehyde, and then permeabilized in buffer A (KPBS supplemented with 2% donkey serum and 0.2% Triton X-100). 293T cells were treated with rabbit anti-Cripto (6900; 1:600) and goat anti-GRP78 (N-20; catalog no. sc-1050; 1:400), while P19 cells were treated with the same anti-Cripto (6900; 1:600) and anti-GRP78 (N-20; catalog no. sc-1050; 1:125) antibodies, together with mouse anti-pan-cadherin (C1821; Sigma; 1/125) in buffer A for 48 h at 4°C. Cells were washed with KPBS and then treated with anti-rabbit, anti-goat, and anti-mouse antibodies, for 1 h at room temperature in buffer A. After further washing in KPBS, the coverslips were mounted in the presence of DAPI (4′,6′-diamidino-2-phenylindole) and then subjected to fluorescence visualization. For confocal images, a Leica TCS SP2 AOBS confocal system (Leica, Wetzlar, Germany) was used. Images were collected using sequential scanning of each excited wavelength to avoid any bleed-through between fluorophores.

Design of lentiviral shRNA vectors and infection of cell lines. Target sequences within the human GRP78 gene were identified and selected using the Sfold program (http://sfold.wadsworth.org/sirna.pl). The design of short hairpin RNA (shRNA) and the production of lentiviral shRNA vectors were carried out as previously described (33). The 83-mer used to generate the GRP78 1 (G1) shRNA was 5′-CTGTCTAGACAAAAAACCATACATTCAAGTTGATTCTC TTGAAATCAACTTGAATGTATGGTCGGGGATCTGTGGTCTCATACA-3′. For viral transduction, lentivirus was produced as previously described (26).

Cell lysates and immunoprecipitations. Cell lysates were prepared in radioimmunoprecipitation assay (RIPA) buffer as previously described (13). For immunoprecipitation experiments, 1 to 5 mg protein extract was precleared by protein G-PLUS-agarose beads for 2 h at 4°C. The precleared extracts were incubated as indicated with 40 μl anti-FLAG M2 gel beads or 20 μl G-PLUS-agarose preincubated with 15 μl anti-GRP78 (KDEL), 10 μl anti-HA, or 25 μl anti-His for 2 h at 4°C. Immunoprecipitates were subsequently washed four times with RIPA buffer and two times with 54K buffer (50 mM Tris, pH 7.9, 150 mM NaCl, 0.5% Triton X-100). We then eluted the proteins either by heating the beads at 95°C in sample buffer or by adding 50 μl of Flag peptide (1 μg/μl), followed by the removal of any remaining associated proteins by heating in sample buffer.

Cell surface biotinylation. Sulfo-NHS-LC-biotin was prepared fresh at 0.5 mg/ml in HEPES dissociation buffer (HDB) and then stored on ice until used. Adherent, intact cells were rinsed twice with ice-cold HDB and then incubated with biotin solution for 30 min on ice by using a sufficient volume to completely cover the cells (e.g., 1 ml/well for six-well plates). The biotinylation reaction was then quenched following the addition of 1 M Tris, pH 7.5, to bring the biotin-HDB solution to a concentration of 50 mM Tris final. The resulting solution was removed, and the cells were rinsed one time in HDB containing 50 mM Tris. Cells were then solubilized in RIPA buffer (50 mM Tris-HCl, pH 7.4, 150 mM NaCl, 1% NP-40, 0.5% deoxycholate, 0.1% sodium dodecyl sulfate [SDS]) supplemented with standard protease inhibitors. Biotinylated proteins were separated by SDS-polyacrylamide gel electrophoresis (PAGE), blotted to nitrocellulose, and then visualized following treatment with avidin-horseradish peroxidase (HRP) and enhanced chemiluminescence.

Cell death assays. For each cell population, three fields each consisting of at least 100 green fluorescent protein (GFP)-positive cells, were scored for apoptotic cells according to their morphologies. The number of cells determined to be apoptotic was divided by the total number of GFP-positive cells in the field, resulting in the percentage of apoptotic cells.

Smad2 phosphorylation and Western blotting. HeLa cells or PC3 cells stably infected with lentivirus were plated on six-well plates at a density of 200,000 cells per well. Forty-eight hours after plating, cells were washed once with HDB and starved for 4 h in additive-free medium and then were left untreated or were treated with TGF-β1 for 30 min. Cells were lysed, and Smad2 phosphorylation assays were carried out by Western blotting as previously described (13).

Cell proliferation assays and colony formation in soft agar. PC3 cells were stably infected with pCSC lentivirus constructs as described above. Cells were plated on 96-well plates at a density of 500 cells/well, and 24 h later, cells were either treated with 10 pM TGF-β1 or left untreated. Eight days after treatment, cell proliferation was measured using the CyQUANT cell proliferation kit according to the manufacturer's instructions. To measure colony formation in soft agar, 96-well plates were prepared with 50 μl/well surface layers consisting of 0.6% agar (Nobel) resuspended in PC3 growth medium. An additional 75 μl/well of 0.33% agar-PC3 growth medium containing 1,000 stably infected PC3 cells was then added to each well, followed by the addition of TGF-β1, which was included in various amounts to yield the specified final concentrations before the agar solidified. Wells were refed with 100 μl of PC3 growth medium with or without TGF-β1 for 15 days, and then colonies were visualized microscopically and counted. Photographs of specified wells were taken using a Canon EOS 400D camera mounted on an inverted Olympus CK40 microscope set to its lowest magnification.

RESULTS

Identification of GRP78 as a novel Cripto binding protein. In order to identify new Cripto-associated proteins, we employed a straightforward strategy in which Cripto was used as bait to "pull down" its binding partners at the cellular membrane. We subjected lysates from 293T cells transfected with empty vector or Cripto-Flag to anti-Flag immunoprecipitation, followed by specific elution of bound proteins with Flag peptide. Since it was carried out under mild conditions, this elution allowed for an additional purification step. As visualized following silver staining, two proteins, migrating at ~72 kDa and

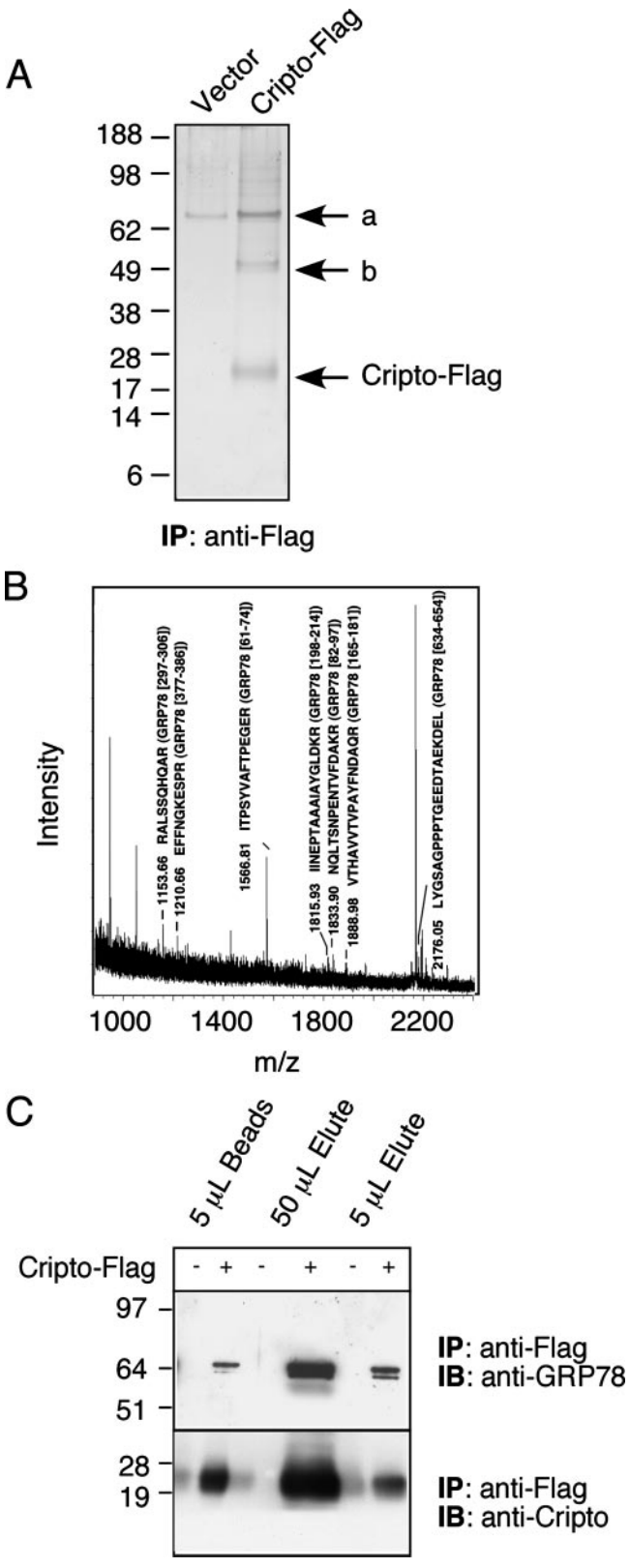

FIG. 1. Identification of novel Cripto binding proteins. 293T cells were transfected with empty vector or Cripto-Flag, subjected to immunoprecipitation on anti-Flag beads, and then eluted with Flag peptide. Cripto-associated proteins were separated by SDS-PAGE and then either silver stained (A) or immunoblotted to nitrocellulose and probed with anti-GRP78 or anti-Cripto antibodies (C) as described in Materials and Methods. Bands a and b in panel A were excised and subjected to mass spectrometric analysis as described in Materials and Methods. Mass fingerprint data corresponding to band a identified as GRP78 are shown in panel B. IB, immunoblot; IP, immunoprecipitate; −, absence of; +, presence of.

~50 kDa, coprecipitated specifically with Cripto-Flag (Fig. 1A, bands a and b, respectively).

We next sought to identify these Cripto-associated proteins by using mass spectrometry. The approximately 72-kDa and 50-kDa bands were excised from the gel, further destained, and subjected to in-gel trypsin digestion. Samples were then analyzed by matrix-assisted laser desorption ionization–time of flight mass spectrometry, and mass fingerprint data were characterized using the Mascot algorithm (Matrix Science, London, United Kingdom). The top hit score of 55 for the band at approximately 72 kDa was for GRP78, also known as BiP, and a total of seven peptides could be assigned in the mass fingerprint with a peptide mass error tolerance of <0.1 Da (Fig. 1B). The band at ~50 kDa (protein b) has not yet been conclusively identified.

GRP78 has multiple functions, including a prominent role in mediating protein folding and the stress response in the ER (18). GRP78 has also been heavily implicated in tumorigenesis (19), and in the present study, we focused on its potential role in binding Cripto and modulating its function. To unequivocally validate the identity of GRP78 as a specific Cripto binding partner, we repeated the coimmunoprecipitation procedure described above and subjected precipitated proteins to Western blotting using specific anti-GRP78 or anti-Cripto antibodies. As shown in Fig. 1C, GRP78 is present in the Flag peptide eluate, indicating that it coimmunoprecipitates specifically with Cripto.

GRP78 binds Cripto at the cell surface. Although GRP78 is thought to function primarily as an ER-associated protein (18), several recent studies have demonstrated that GRP78 is also expressed at the plasma membranes of cancer cells under certain conditions (19). In order to test whether Cripto and GRP78 interact at the cell surface, we labeled intact cells with a cell-impermeable biotin reagent and subjected resulting cell lysates to anti-Flag immunoprecipitation, followed by elution with Flag peptide and the detection of biotinylated proteins with avidin. As a negative control, we used a ~26-kDa transmembrane fragment of the p75 neurotrophin receptor referred to as p26-Flag. This irrelevant protein is similar in size to Cripto and was subjected to the same procedure, side by side with Cripto-Flag. As shown in Fig. 2A, biotinylated forms of GRP78 and protein b coimmunoprecipitated with Cripto, but not with p26, suggesting that the association of Cripto with GRP78 and protein b is specific. The fact that GRP78 and Cripto were biotinylated indicates that they interact at the cell surface and diminishes the likelihood that their association depends on the chaperone activity of GRP78.

To further characterize the ability of Cripto to bind cell surface GRP78, we tested whether GRP78 from one population of cells could bind mature Cripto isolated from a separate cell population in a cell-free system. 293T cells were infected

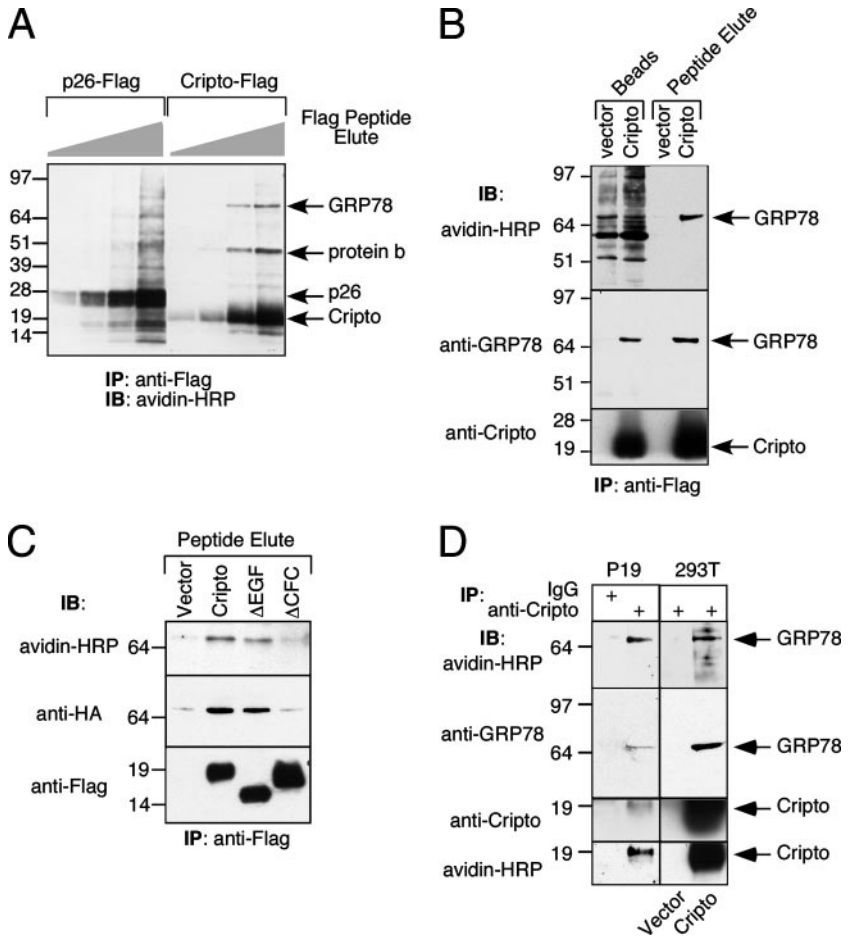

FIG. 2. Cripto binds GRP78 at the cell surface. 293T cells transfected with the indicated constructs (A to D) and P19 cells (D) were labeled with cell-impermeable NHS-LC-biotin. Cell lysates were subjected to immunoprecipitation by using the indicated antibodies and then eluted with Flag peptide (peptide elute) or by heating the beads in sample buffer. Samples were resolved via SDS-PAGE and blotted with avidin-HRP or the indicated antibodies as described in Materials and Methods. In some cases (B and C), 293T cells overexpressing GRP78 were subjected to cell surface biotinylation and then resulting cell lysates were incubated with vector or Cripto-Flag beads. IB, immunoblot; IgG, immunoglobulin G; IP, immunoprecipitate; +, presence of.

with vector or Cripto-Flag and then subjected to anti-Flag immunoprecipitation, followed by extensive washing of the beads. In parallel, a separate population of 293T cells infected with GRP78 was subjected to cell surface biotinylation and lysates from these cells were incubated with the beads previously incubated with vector or Cripto-Flag lysates. The beads were then washed again, and bound proteins were eluted with Flag peptide and subjected to Western blotting using avidin-HRP, anti-GRP78, or anti-Cripto antibodies. As shown in Fig. 2B, Flag peptide specifically eluted Cripto-Flag, together with the majority of bound GRP78. Moreover, biotinylated (i.e., cell surface-labeled) GRP78 was specifically eluted from beads previously exposed to Cripto-Flag lysates, but not from beads exposed to vector lysates. These results demonstrate that the interaction between cell surface-derived GRP78 and Cripto occurs in vitro in a manner that is independent of cellular or membranal contexts. In addition, since biotinylated GRP78 and Cripto originated from separate cell populations, their interaction does not depend on prior association in the ER, on the translational machinery, or any chaperone function of GRP78.

Cripto possesses two modular domains that mediate protein-protein interactions, an EGF-like domain and a cysteine-rich CFC domain (34). In order to explore the interaction between Cripto and GRP78 further, we used the method described above (Fig. 2B) to test whether cell surface-labeled GRP78 binds Cripto mutants lacking either the EGF-like domain (ΔEGF) or the CFC domain (ΔCFC). In this experiment, we assessed the ability of biotinylated, HA-tagged GRP78 from one cell population to bind wild-type and mutant forms of Cripto originating from separate cell populations. As shown in Fig. 2C, cell surface GRP78 bound wild-type Cripto and the Cripto ΔEGF mutant to similar extents, but it did not bind the Cripto ΔCFC mutant. Therefore, this result indicates that cell surface-derived GRP78 binds the CFC domain of Cripto.

Having shown that overexpressed Cripto and GRP78 bind at the cell surface in a specific manner that depends on the CFC domain of Cripto, we next tested whether these two proteins

are associated in an endogenous setting. Embryonal carcinoma cell lines were reported to express high levels of Cripto protein, and we tested whether endogenous Cripto and endogenous GRP78 interact in mouse embryonal carcinoma P19 cells. We treated these cells with membrane-impermeable biotin as described above and subjected lysates to immunoprecipitation with anti-Cripto antibody or rabbit immunoglobulin G (IgG) as a negative control. As a positive control for the immunoprecipitation, we used 293T cells infected with empty vector or Cripto-Flag. As shown in Fig. 2D, anti-Cripto immunoprecipitation from P19 cells, followed by anti-GRP78 Western blotting, led to the detection of a band corresponding to GRP78, while precipitation with nonimmune IgG failed to do so. Furthermore, the precipitated Cripto and GRP78 proteins were biotinylated, as indicated by their detection with avidin-HRP, indicating that they originated from the cell surface. A similar result was obtained with 293T cells overexpressing Cripto-Flag, but not with empty vector cells (Fig. 2D, right panel), validating the specificity of the anti-Cripto antibody. Therefore, endogenous Cripto and endogenous GRP78 specifically interact at the cell surfaces of mouse embryonal carcinoma P19 cells and their interaction does not require the overexpression of either protein.

Cripto and GRP78 colocalize at the cell surface. We further assessed the cellular localization of these proteins by immunofluorescence and confocal microscopy. Initially, 293T cells infected with empty vector or coinfected with Cripto and GRP78 were stained with anti-Cripto and anti-GRP78 antibodies. As shown in Fig. 3A, vector cells displayed minimal background level Cripto staining and weak GRP78 staining, resulting from the presence of the endogenous protein. By contrast, 293T cells overexpressing Cripto and GRP78 gave rise to prominent, punctate staining of both proteins, with striking colocalization at the cell surface (Fig. 3A). Although the significance of the punctate structures remains to be determined, this result clearly demonstrates the association of overexpressed Cripto and GRP78 at the plasma membranes of intact 293T cells.

Next, we tested whether Cripto and GRP78 are similarly associated at the cell surfaces when expressed at endogenous levels in P19 cells. As shown in Fig. 3B, both Cripto and GRP78 were readily detected in native P19 cells. These cells were also stained with an anti-pan-cadherin antibody that was used as a marker of the plasma membrane. Overall, the staining for Cripto and GRP78 appeared to be predominantly punctate/vesicular in nature, with partial but substantial colocalization. Importantly, several of the punctate structures containing both Cripto and GRP78 displayed overlapping staining with pan-cadherin, placing them at the plasma membranes of these cells (Fig. 3B, inset). The colocalization of Cripto and GRP78 both at the membrane and within vesicular structures suggests that they associate not only at the plasma membrane but also during the endosomal/lysosomal trafficking and recycling commonly associated with cell surface signaling proteins.

Cripto-associated GRP78 can be targeted using shRNA. Having demonstrated that Cripto and GRP78 are associated cofactors at the cell surface, we next aimed to determine whether GRP78 modulates known Cripto functions. To this end, we developed shRNAs capable of reducing endogenous GRP78 expression. GRP78 is induced by thapsigargin, a compound that raises cytosolic calcium levels, causes ER stress, and triggers apoptosis. Following thapsigargin treatment, GRP78 induction alleviates ER stress and delays the cellular apoptotic response (15). Therefore, we initially tested the ability of an shRNA targeting GRP78 (G1) to prevent the induction and function of GRP78 following thapsigargin treatment. As shown by Western blot analysis using anti-GRP78 antibody, thapsigargin clearly induced GRP78 expression in HeLa cells and this induction was blocked by the G1 shRNA (Fig. 4A). Furthermore, as shown in Fig. 4B, G1-infected HeLa cells showed a marked increase in thapsigargin-induced apoptosis in comparison to vector cells, demonstrating the functional consequences of GRP78 knockdown by this shRNA.

We next examined whether the G1 shRNA could similarly target the cell surface pool of GRP78 associated with Cripto. HeLa cells infected with empty vector or G1 shRNA were subsequently infected with Cripto-Flag. These cells were then subjected to cell surface biotinylation, followed by anti-Flag immunoprecipitation and specific elution with Flag peptide as previously described. Eluted proteins were subsequently analyzed by Western blotting using avidin-HRP, anti-GRP78, or anti-Cripto antibodies. As shown in Fig. 4C, the amount of cell surface-biotinylated GRP78 that coimmunoprecipitated with Cripto was substantially reduced in the presence of the G1 shRNA construct. Importantly, this result indicates that the G1 shRNA can disrupt functions of GRP78-Cripto complexes at the cell surface.

Targeted reduction of GRP78 expression enhances TGF-β-dependent Smad2 phosphorylation. We previously demonstrated that shRNA knockdown of endogenous Cripto in HeLa cells causes an increase in TGF-β-induced Smad2 phosphorylation (13). Here we have shown that GRP78 and Cripto interact at the cell surface, raising the possibility that Cripto and GRP78 work in concert to inhibit TGF-β signaling. Having demonstrated that the G1 shRNA effectively targets the Cripto-associated pool of GRP78 at the plasma membrane, we next tested whether it, similar to the Cripto shRNA, could enhance TGF-β signaling. Once again, the same HeLa cells infected with empty vector or G1 were tested in the absence (Fig. 5A) or presence (Fig. 5B) of 5 μM thapsigargin. In each case, cells were treated with a range of TGF-β1 doses and resulting levels of phospho-Smad2 and total Smad2 were monitored. As shown in Fig. 5A, G1 shRNA cells were more responsive to TGF-β than vector-infected cells at lower doses (e.g., 1 pM TGF-β1). Following thapsigargin treatment, the TGF-β dose-response relationship was shifted substantially to the right (Fig. 5B). Again, cells infected with G1 had a greater sensitivity to TGF-β, with a prominent phospho-Smad2 band detected at 10 pM TGF-β1. Interestingly, the G1 shRNA effect of sensitizing cells to TGF-β was more pronounced in the presence of thapsigargin than in its absence. This result suggests that the induction of cell surface GRP78 by thapsigargin causes an inhibition of TGF-β signaling that can be blocked by the G1 shRNA construct.

To test whether thapsigargin causes the induction of cell surface GRP78 that is targeted by G1, the same HeLa cells infected with vector or G1 were treated with vehicle or thapsigargin and then subjected to cell surface biotinylation. To visualize biotinylated GRP78, cell lysates were subjected to immunoprecipitation with anti-GRP78 antibody, followed by Western blotting with avidin-HRP. As shown in Fig. 5C, thap-

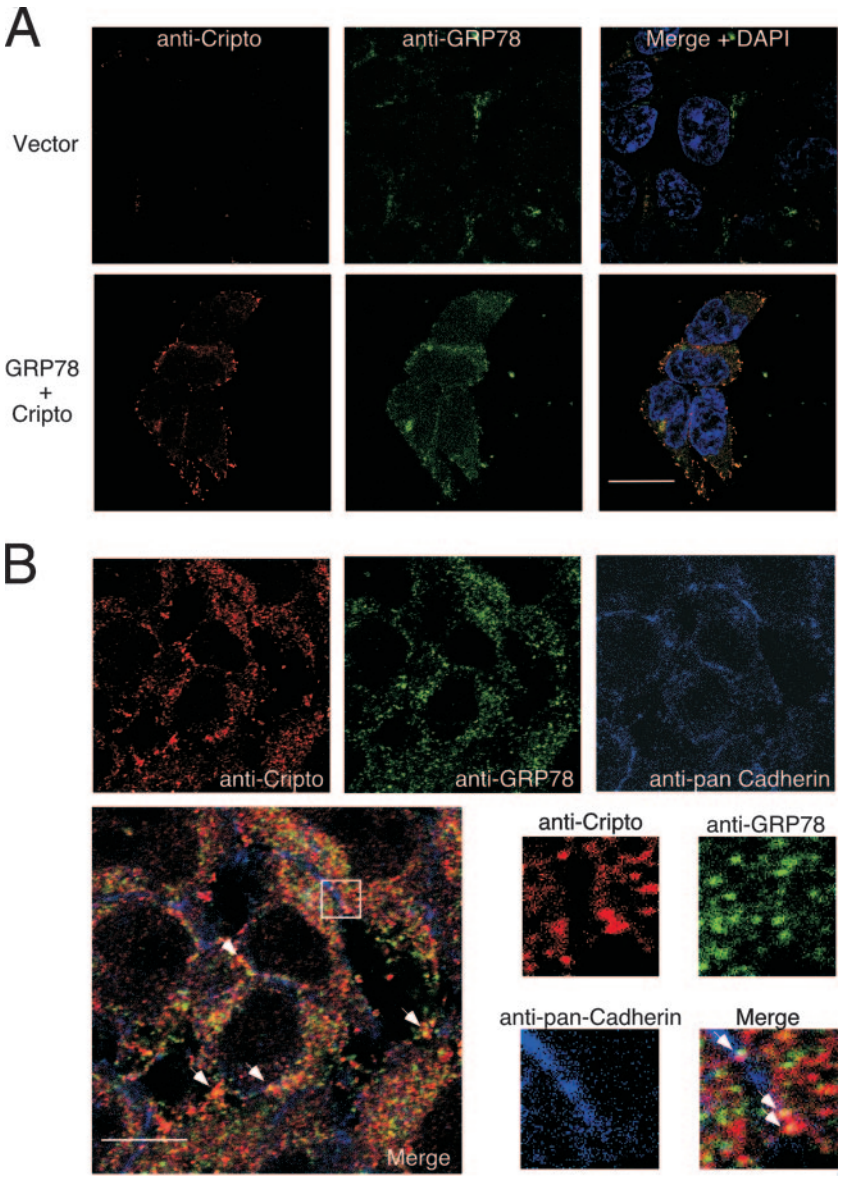

FIG. 3. Cripto and GRP78 colocalize at the cell surface. (A) 293T cells stably infected with vector or GRP78 and Cripto (GRP78 + Cripto) were stained with anti-Cripto antibody (red) and anti-GRP78 antibody (green) as described in Materials and Methods. Scale bar = 20 μm. (B) P19 cells were stained with the same anti-Cripto (red) and anti-GRP78 (green) antibodies as in panel A and anti-pan-cadherin antibody (blue) as described in Materials and Methods. Magnified images corresponding to the boxed region are presented to highlight colocalization of Cripto, GRP78, and cadherin proteins. Scale bar = 10 μm. All cells were analyzed using confocal microscopy as described in Materials and Methods.

sigargin treatment induced GRP78 at the cell surface and this induction was blocked by the G1 shRNA construct. Finally, as an additional control, we tested whether GRP78 knockdown or induction results in altered levels of type I and/or type II TGF-β signaling receptors. As shown in Fig. 5D, neither the presence of G1 shRNA nor treatment with thapsigargin significantly affected receptor levels, with one exception being that TβRI levels were slightly higher in vector cells than in G1 cells in the absence of thapsigargin. This discrepancy did not correlate with TGF-β signaling, however, since phospho-Smad2 levels were higher in G1 cells than in vector cells (Fig. 5A). Thus, GRP78 does not appear to affect TGF-β signaling by altering the levels of these receptors. In summary, these data indicate for the first time that in a manner similar to that of endogenous Cripto, endogenous GRP78 inhibits TGF-β signaling. Furthermore, these findings are consistent with a novel role for cell surface GRP78-Cripto complexes in blocking TGF-β signaling.

GRP78 does not directly bind TGF-β signaling receptors. Our finding that GRP78 inhibits TGF-β signaling raised the possibility that it does so by binding directly to type I and/or type II TGF-β signaling receptors. We have shown above that endogenous cell surface GRP78 coimmunoprecipitates with Cripto when Cripto is overexpressed in 293T cells and with endogenous Cripto in P19 cells. Here we have further tested whether GRP78 similarly coimmunoprecipitates with TβRI

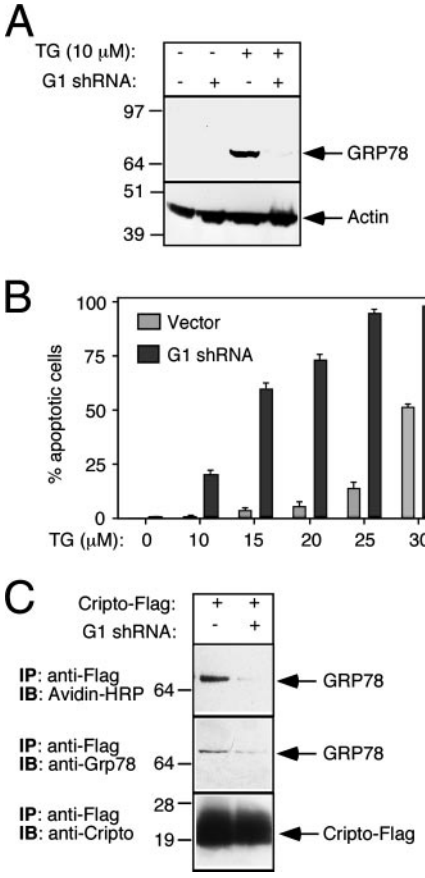

FIG. 4. Targeted reduction of GRP78 expression using RNA interference. HeLa cells were infected with lentivirus containing either GRP78 shRNA (G1) or empty vector and were either left untreated or treated with thapsigargin as indicated. (A) Cell lysates were analyzed by Western blotting using anti-GRP78 or anti-actin antibodies as described in Materials and Methods. (B) Bars represent the number of apoptotic cells per 100 GFP-positive cells as described in Materials and Methods. Error bars indicate standard deviations. (C) Cells infected with vector or G1 shRNA virus were reinfected with virus containing Cripto-Flag. Lysates from these cells were subjected to immunoprecipitation by using anti-Flag beads and then eluted with Flag peptide. Eluted proteins were subjected to Western blot analysis using avidin-HRP, anti-GRP78, and anti-Cripto as described in Materials and Methods. IB, immunoblot; IP, immunoprecipitate; TG, thapsigargin; −, absence of; +, presence of.

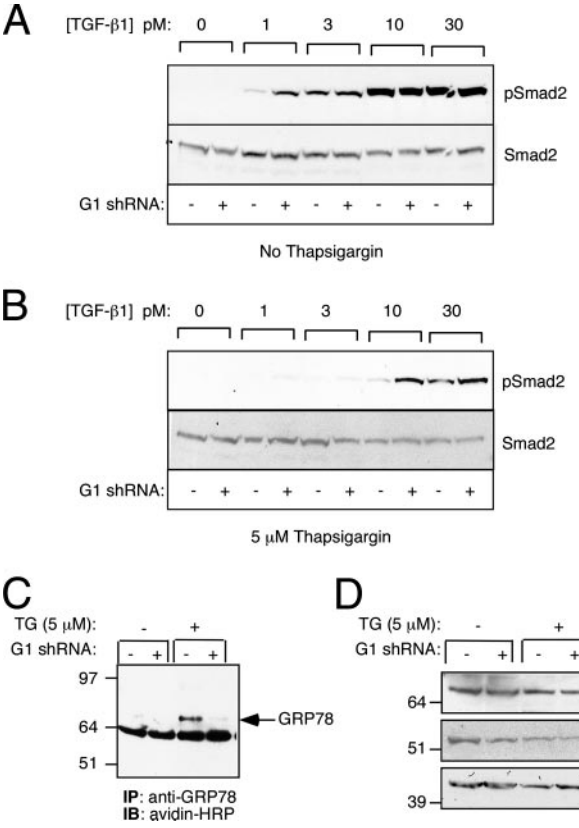

FIG. 5. Inhibition of endogenous GRP78 expression enhances TGF-β-induced Smad2 phosphorylation. HeLa cells were infected with lentivirus containing either shRNA (G1) targeted against GRP78 or empty vector and were then left untreated or treated with 5 μM thapsigargin as indicated. Following overnight thapsigargin treatment, cells were treated with the indicated doses of TGF-β1 (A and B) and then phospho-Smad2 and total Smad2 levels were determined by Western blot analysis as described in Materials and Methods. Alternatively, the same cells treated as indicated were labeled with cell-impermeable biotin with resulting lysates subjected to immunoprecipitation with anti-GRP78 antibodies (anti-KDEL), followed by Western blotting using avidin-HRP (C), or lysates were subjected directly to Western blotting using anti-TβRI, anti-TβRII or anti-actin antibodies (D) as described in Materials and Methods. IP, immunoprecipitate; TG, thapsigargin; −, absence of; +, presence of.

and TβRII. 293T cells were transfected with p26-Flag, Cripto-Flag, TβRI-HA, or TβRII-His, and surface proteins were biotinylated as before. Each of these proteins was immunoprecipitated as bait, and then immune complexes were assessed for the presence of GRP78. As shown in Fig. 6, the avidin-HRP panel reflects the fact that similar amounts of these different cell surface bait proteins were precipitated in these pull-downs. However, only Cripto pulled down endogenous GRP78, as detected by both avidin-HRP and anti-GRP78 antibody (Fig. 6). Therefore, under these conditions, cell surface GRP78 does not bind TβRI or TβRII but rather appears to associate exclusively with Cripto. This result suggests that the effect of GRP78 on TGF-β signaling is not likely to occur via its direct independent binding to either signaling receptor.

Cripto and GRP78 cooperate to inhibit TGF-β signaling. TGF-β has been shown to inhibit both anchorage-dependent and anchorage-independent growth of human prostate carcinoma PC3 cells (39). Therefore, we tested whether Cripto and GRP78 work together to modify TGF-β effects in these cells. First, we tested the effects of Cripto and GRP78 on TGF-β-dependent Smad2 phosphorylation. As shown in Fig. 7A, treatment of vector-infected cells with 10 pM TGF-β1 resulted in Smad2 phosphorylation and this effect was moderately attenuated when GRP78 or Cripto was overexpressed separately. When cells were infected with both Cripto and GRP78, however, the TGF-β effect was inhibited to a much greater extent. The intensities of the phospho-Smad2 bands presented in Fig. 7A were then quantitated and normalized to corresponding total Smad2 levels (Fig. 7B). This quantitation shows that TGF-β signaling was inhibited in cells expressing GRP78 or Cripto by about 40% and ~43%, respectively. By contrast, cells

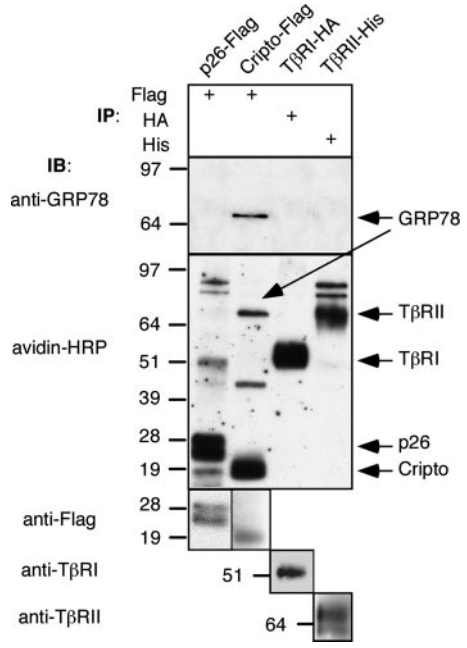

FIG. 6. GRP78 does not bind directly to TGF-β type I and type II receptors. 293T cells were transfected with p26-Flag, Cripto-Flag, TβRI-HA, or TβRII-His and then subjected to immunoprecipitation using anti-Flag, anti-HA, or anti-His antibodies as indicated. Precipitated proteins were analyzed via Western blotting using avidin-HRP or the indicated antibodies as described in Materials and Methods. IB, immunoblot; IP, immunoprecipitate; +, presence of.

coexpressing GRP78 and Cripto together showed a reduction of about 74% in TGF-β-induced Smad2 phosphorylation. Next, we tested whether the overexpression of Cripto and/or GRP78 affected the levels of TGF-β signaling receptors in these cells. As shown in Fig. 7C, the levels of these receptors were not significantly altered (Fig. 7C). Together, these data further support a novel role for GRP78 as a TGF-β antagonist and indicate that Cripto and GRP78 function cooperatively to inhibit TGF-β signaling.

Next, we measured the relative proliferation rates of infected PC3 cell populations in the absence or presence of 10 pM TGF-β1. As shown in Fig. 7D, TGF-β1 treatment of vector-infected cells reduced proliferation by about 58%, while the treatment of cells expressing GRP78 or Cripto alone reduced proliferation by about 42% and 19%, respectively. Again, when GRP78 and Cripto were expressed together in these cells, the effect was stronger. Interestingly, TGF-β1 treatment in this case actually resulted in an increase in cellular proliferation of about 31% (Fig. 7C). Importantly, the data presented here demonstrate that while GRP78 and Cripto each attenuate the antiproliferative effects of TGF-β, their coexpression, which allows for their physical interaction, creates conditions that cause TGF-β to enhance cellular growth.

GRP78 and Cripto collaborate to block the antiproliferative effects of TGF-β. Finally, we tested the effects of GRP78 and Cripto on anchorage-independent growth in the presence or absence of TGF-β1. The same PC3 cells infected with empty vector, GRP78, Cripto, or both were seeded in soft agar in the presence of escalating doses of TGF-β1, and colonies were allowed to grow for 15 days. As shown in Fig. 8A, TGF-β1 inhibited colony formation in a dose-dependent manner. In order to highlight the relative effects of TGF-β on each cell population, the same data are also presented as the number of colonies in the presence of TGF-β1 normalized to the number of colonies in its absence (Fig. 8B). Two major conclusions can be drawn from these data. First, in the absence of TGF-β treatment, cells expressing either GRP78 or Cripto formed more colonies than did vector cells and this increase was largely enhanced in cells expressing both GRP78 and Cripto (Fig. 8A). Second, while GRP78 and Cripto each have some ability to block the growth-inhibitory effects of TGF-β individually, they have a much greater ability to do so when expressed together (Fig. 8B). The extent to which coexpression of GRP78 and Cripto attenuated the growth-inhibitory effect of TGF-β is further illustrated by photographs of these colonies. As shown in Fig. 8C, 100 pM TGF-β1 was sufficient to dramatically reduce colony formation of vector-infected cells and had a similar but weaker inhibitory effect on cells expressing either Cripto or GRP78 individually. By contrast, cells expressing both GRP78 and Cripto together appeared to be more refractory to the cytostatic effects of TGF-β, as illustrated by both the number and the sizes of the colonies. Once again, these data support a cooperative function for GRP78 and Cripto in blocking TGF-β inhibition of anchorage-independent growth.

Figure 8D depicts a model in which GRP78 and Cripto function as cell surface binding partners to restrict TGF-β-dependent growth inhibition and to promote cell proliferation. Our data indicate that Cripto and GRP78 carry out these functions in a cooperative manner, presumably as a complex, since they physically interact and since their effects were cooperatively enhanced. However, our data do not completely rule out the possibility that these proteins can partly inhibit TGF-β signaling and cause enhanced proliferation on their own. Finally, in addition to its ability to activate cytostatic signaling, TGF-β itself has been reported to activate survival pathways under certain conditions. This report coincides with our observation that TGF-β causes enhanced proliferation of PC3 cells only when the cells coexpress both Cripto and GRP78 (Fig. 8D).

DISCUSSION

In the present study, we have identified GRP78 as a novel Cripto binding partner and shown that these two proteins form a cell surface complex that inhibits cytostatic TGF-β signaling and promotes tumor cell growth. GRP78 has been extensively characterized as an ER chaperone that assists in protein folding, maturation, and assembly and also coordinates the unfolded protein response (3, 17, 18). GRP78 is induced under conditions of hypoxia and nutrient deprivation, and it is therefore not surprising that it is found at high levels in tumor cells (19). Evidence for a necessary role for GRP78 in tumor progression first emerged from the elegant demonstration that the inhibition of GRP78 induction in fibrosarcoma cells with antisense rendered them completely incapable of forming tumors in nude mice without affecting their growth in vitro (15). Moreover, the delivery of a suicide transgene driven by the GRP78 promoter into fibrosarcoma and breast tumor cells caused complete eradication of sizable tumors in mice (6, 10, 11).

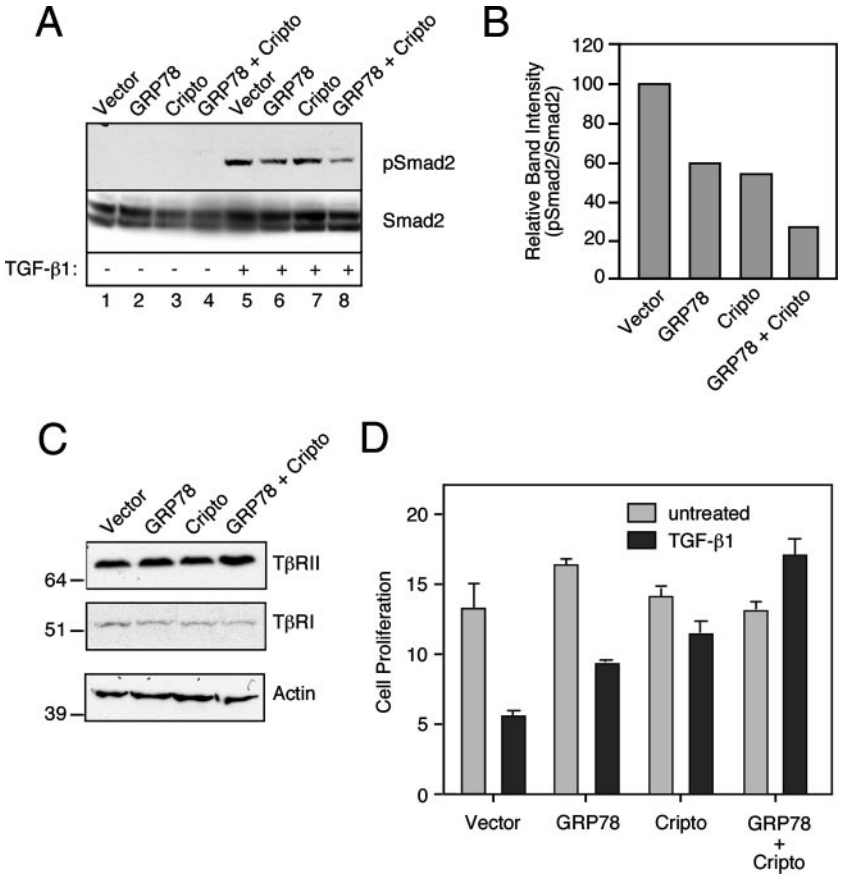

FIG. 7. Cripto and GRP78 cooperate to inhibit TGF-β signaling. (A) PC3 cells infected with empty vector, GRP78, Cripto, or both were either left untreated or treated with TGF-β1 (10 pM) as indicated. Phospho-Smad2 (pSmad2) and total Smad2 (Smad2) levels were determined by Western blot analysis as described in Materials and Methods. (B) Phospho-Smad2 bands from panel A were quantitated using densitometry and normalized relative to corresponding Smad2 bands as described in Materials and Methods. (C) PC3 cell lysates were subjected to Western blotting using anti-TβRII, anti-TβRI, and anti-actin antibodies as indicated and as described in Materials and Methods. (D) Cells were plated on 96-well plates, and then cell proliferation was measured 8 days later as described in Materials and Methods. Error bars indicate standard deviations. −, absence of; +, presence of.

Thus, the environment found within solid tumors causes the induction of GRP78 and its expression facilitates tumor growth.

Although GRP78 resides predominantly within the ER, it can exist as a transmembrane protein (28) and is localized to the plasma membrane in tumor cells as was initially demonstrated in human rhabdomyosarcoma cells following treatment with thapsigargin (8, 9). Subsequently, global profiling of the cell surface proteome has confirmed that GRP78 is surface exposed on tumor cells (31). Indeed, GRP78 has been shown to function, together with major histocompatibility complex class I, at the cell surface as a coreceptor for viruses (36) and to act as a receptor for plasminogen-derived Kringle 5 domain (7) and activated α_2-macroglobulin (23, 24). Of note, GRP78 receptor function was shown to cause the activation of growth pathways, leading to increased cellular proliferation and anti-apoptotic behavior (21, 22, 24). Such a receptor function of GRP78 draws cancer-related relevance from the observation that the presence of autoantibodies to GRP78 has been linked to increased prostate cancer progression and decreased patient survival (20). Moreover, a causal role for GRP78 in the progression of cancer was supported by the finding that suicide peptides targeting GRP78 at the plasma membrane were demonstrated to selectively kill tumor cells (2). Importantly, these findings validate cell surface GRP78 as a putative target for cancer therapy.

GRP78 and Cripto form a complex at the cell surface that does not require prior association in the ER. We have shown here that GRP78 forms a complex with Cripto at the cell surface, a discovery with functional as well as potential therapeutic implications. This interaction appears to be specific and exclusive, since GRP78 was one of only two cell surface proteins observed to copurify with Cripto and since an irrelevant transmembrane protein similar in size to Cripto did not copurify with GRP78. Likewise, both type I and type II TGF-β receptors were unable to immunoprecipitate GRP78 under the same conditions. Our results also indicate that Cripto/GRP78 binding does not depend on GRP78 ER chaperone function since their interaction was observed in a cell-free environment following the maturation and processing of these proteins within separate cell populations. This result also supports the existence of this complex at the cell surface since the GRP78 shown to bind Cripto under these conditions was derived from the plasma membrane. Furthermore, this result suggests that

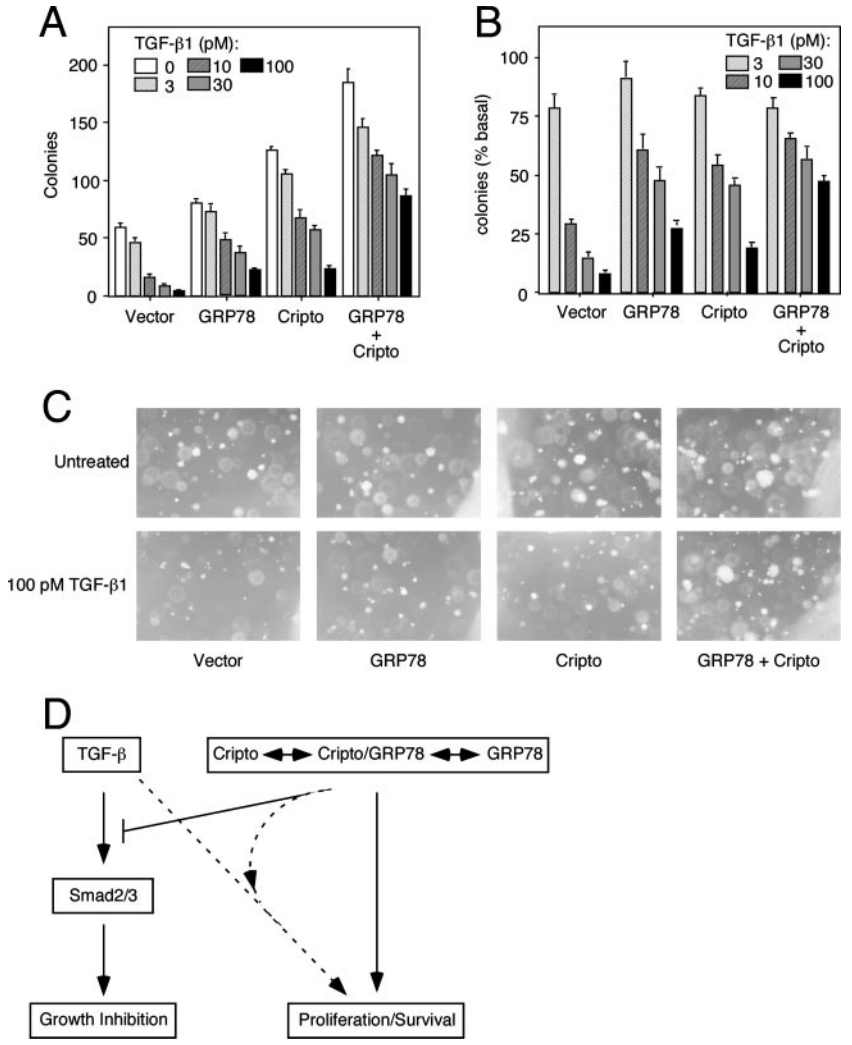

FIG. 8. GRP78 and Cripto collaborate to inhibit the antiproliferative effects of TGF-β on anchorage-independent growth of prostate carcinoma cells. PC3 cells infected with vector, GRP78, Cripto or both were grown for 15 days under anchorage-independent conditions in soft agar in the presence of either vehicle or escalating doses of TGF-β1 as described in Materials and Methods. Data are presented as the number of colonies counted within a single field in the absence or presence of the indicated doses of TGF-β1 (A) or as the number of colonies counted in the presence of the indicated TGF-β1 concentrations divided by the number of colonies counted in the absence of TGF-β1 treatment (% basal) (B). (C) Photographs taken from the indicated fields either in the presence of 100 pM TGF-β1 or in its absence. (D) Model illustrating oncogenic function of Cripto/GRP78 complex. TGF-β potently inhibits proliferation of many cell types by signaling via the Smad2/3 pathway (left). Cripto and GRP78 interact to form a complex and act cooperatively to attenuate TGF-β-dependent Smad signaling and growth inhibition. In addition, they independently increase cell proliferation/survival. In the presence of Cripto and GRP78, TGF-β can also increase cellular proliferation (dashed arrow). Error bars indicate standard deviations.

the information required for this specific binding interaction may be contained in full within the tertiary structures of these two proteins and it raises the possibility of targeting tumor cells through the future development of molecules that specifically disrupt their interaction.

Similar to what we have observed with overexpressed proteins, we found that endogenous Cripto and endogenous GRP78 could be isolated as a complex originating from the surfaces of mouse embryonal carcinoma cells. This finding further supports an intrinsic role for their interaction as signaling cofactors at the plasma membrane and again argues against the possibility that GRP78 simply plays a role in the folding of overexpressed Cripto in the ER. We have also explored the localization of Cripto and GRP78 in the same cells via immunocytochemistry, and interestingly, we found that Cripto and GRP78 were predominantly colocalized in punctate structures, a portion of which were present at the cell surface. This finding supports our conclusion that Cripto and GRP78 function together at the plasma membrane, but it also indicates that they are associated during vesicular transport, as is common for signaling proteins. In addition, the punctate nature of the cell surface staining is consistent with previous reports showing both of these proteins to associate with lipid rafts (37, 38). Future research will now be aimed at characterizing the exact nature, contents, and dynamics of these cell surface structures.

GRP78 binds the CFC domain of Cripto. The specificity of the interaction between Cripto and GRP78 was further sup-

ported by our demonstration that the CFC domain of Cripto appeared to be both necessary and sufficient for GRP78 binding. This finding is also noteworthy since it suggests that Cripto may bind TGF-β via its EGF-like domain, as we have previously shown (13), while simultaneously binding GRP78 via its CFC domain. We speculate that larger-order protein complexes containing Cripto, GRP78, TGF-β, and TGF-β receptors may also form and result in reduced and/or altered TGF-β signaling. In addition, our observation that the CFC domain of Cripto binds GRP78 has further relevance with regard to possible effects of GRP78 on Cripto modulation of signaling by other TGF-β ligands, such as Nodal and activins. For example, it has previously been shown that the CFC domain of Cripto specifically binds the activin/Nodal type I receptor ALK4 (40) and GRP78 may therefore compete with ALK4 for Cripto binding. Alternatively, GRP78 may participate in protein complexes containing ALK4, Cripto, and activin/Nodal. Future mechanistic studies will now be directed toward further characterizing the role of GRP78 in modulating Cripto effects on signaling by these TGF-β ligands.

Targeted knockdown of Cripto-associated GRP78 inhibits TGF-β signaling. As outlined above, multiple lines of evidence have shown that Cripto and GRP78 each promote tumorigenesis and both proteins are selectively expressed at the cell surfaces of cancer cells. The novelty of the present study, however, stems from the discovery that these two proteins, both of which have previously been implicated in the promotion of tumor growth, form a complex at the cell surface. This discovery links these proteins physically and also mechanistically via the inhibition of TGF-β signaling.

Initially, we studied the role of GRP78 in TGF-β signaling by developing an shRNA capable of reducing the levels of GRP78 associated with Cripto at the plasma membrane. Interestingly, this shRNA enhanced TGF-β-dependent Smad2 phosphorylation, providing evidence that endogenous GRP78 can restrict TGF-β signaling. To our knowledge, this finding represents the first demonstration that GRP78 affects TGF-β signaling and, significantly, it constitutes a novel mechanism through which cell surface GRP78 may convey its tumorigenic message. This result also coincides with the previous demonstration that endogenous Cripto has a similar role in these cells (13) and is consistent with the hypothesis that GRP78 binds Cripto at the cell surface to antagonize growth-inhibitory TGF-β signaling.

GRP78 and Cripto cooperate to attenuate cytostatic TGF-β signaling and enhance proliferation in human prostate carcinoma cells. Our demonstration that GRP78 and Cripto inhibit TGF-β-dependent Smad2 phosphorylation to a greater extent when expressed together than when expressed separately indicates that they function together to inhibit TGF-β signaling. Also, since the level of Smad phosphorylation depends directly on the extent of receptor activation, this result suggests that Cripto and GRP78 exert their inhibitory effect by reducing the ability of TGF-β to activate its receptors. Such an interpretation is further supported by the fact that the overexpression of Cripto and/or GRP78 in these cells does not alter TGF-β receptor levels. Furthermore, our inability to detect a direct interaction between GRP78 and either type I or type II TGF-β receptors suggests that GRP78 may exert its inhibitory effect on TGF-β signaling by binding Cripto or by directly binding TGF-β or both Cripto and TGF-β.

We have further shown that Cripto and GRP78 function cooperatively to enhance cell growth and inhibit the cytostatic effects of TGF-β. When cells were grown under anchorage-dependent conditions, Cripto and GRP78 each attenuated the growth-inhibitory effects of TGF-β and, interestingly, their coexpression caused TGF-β to switch from being antiproliferative to being pro-proliferative in nature. Although the mechanism underlying this joint effect of Cripto and GRP78 on the proliferative response of cells to TGF-β remains to be determined, TGF-β was shown to increase proliferation/survival under conditions in which its cytostatic effects have been lost (27). Likewise, we found that Cripto and GRP78 had a cooperative ability to block the cytostatic effects of TGF-β under anchorage-independent conditions. However, unlike what was observed in monolayers, TGF-β treatment did not enhance the growth of cells coexpressing Cripto and GRP78 in soft agar. Another difference was that GRP78 and Cripto increased colony growth in soft agar in the absence of TGF-β treatment both when expressed separately and, more prominently, when coexpressed.

Therefore, our results indicate that GRP78 and Cripto influence cell growth and TGF-β responsiveness in a manner that varies depending on the specific growth conditions. This result is not surprising in light of the distinct signaling pathways activated in response to the environment in cells grown under anchorage-dependent as opposed to anchorage-independent conditions. For example, tumor cells utilize signaling pathways, such as FAK and Src, to facilitate anchorage-independent growth and avoid anoikis (25). Thus, although the specific mechanisms remain to be elucidated, the convergence of signals emanating from TGF-β with signaling pathways specifically associated with a particular growth setting can lead to nuances in growth effects. Despite the differences we observed, we consistently found the effects of Cripto and GRP78 on TGF-β responsiveness to be greater when both proteins were expressed together than when each was expressed individually. Thus, cell surface Cripto-GRP78 complexes displayed a clear and consistent role in inhibiting cytostatic TGF-β responses under both anchorage-dependent and -independent growth conditions.

TGF-β is a major tumor suppressor, and the loss of its cytostatic function is associated with tumor initiation and progression (27). This loss of growth-inhibitory TGF-β signaling may result from the reduction of receptor signaling, impaired Smad function, or the disruption of the transcriptional regulators or their targets that together constitute the cytostatic program (32). Indeed, TGF-β signaling frequently exacerbates the growth and spread of tumors that are resistant to its antiproliferative effects (27). Cripto and GRP78 have each been implicated separately in human cancer progression, and each of these proteins is selectively expressed on the surfaces of tumor cells. Here we have provided the first evidence that these two proteins physically interact at the cell surface. We have further provided the first demonstration that they cooperate to enhance tumor cell growth and reverse the tumor suppressor effects of TGF-β. We propose that this complex leads to increased malignancy and that it confers a competitive proliferative advantage to tumor cells via inhibition of TGF-β sig-

naling at the receptor level. In light of these findings, the cell surface Cripto-GRP78 complex may represent a desirable target with significant therapeutic potential because of its intrinsic selective advantage of affecting only cancer cells but not their normal tissue counterparts.

ACKNOWLEDGMENTS

We thank Dave Dalton for his assistance in preparing the manuscript.

This work was supported by grant number R01CA107420 from the National Cancer Institute, the Foundation for Medical Research, Inc., the Robert J. Jr. and Helen C. Kleberg Foundation, the Vincent J. Coates Foundation, and the International Human Frontier Science Program Organization. W. Vale is a senior investigator of the Foundation for Medical Research, Inc.

REFERENCES

1. **Adkins, H. B., C. Bianco, S. G. Schiffer, P. Rayhorn, M. Zafari, A. E. Cheung, O. Orozco, D. Olson, A. De Luca, L. L. Chen, K. Miatkowski, C. Benjamin, N. Normanno, K. P. Williams, M. Jarpe, D. LePage, D. Salomon, and M. Sanicola.** 2003. Antibody blockade of the Cripto CFC domain suppresses tumor cell growth in vivo. J. Clin. Investig. **112:**575–587.
2. **Arap, M. A., J. Lahdenranta, P. J. Mintz, A. Hajitou, A. S. Sarkis, W. Arap, and R. Pasqualini.** 2004. Cell surface expression of the stress response chaperone GRP78 enables tumor targeting by circulating ligands. Cancer Cell **6:**275–284.
3. **Bernales, S., F. R. Papa, and P. Walter.** 2006. Intracellular signaling by the unfolded protein response. Annu. Rev. Cell Dev. Biol. **22:**487–508.
4. **Bianco, C., S. Kannan, M. De Santis, M. Seno, C. K. Tang, I. Martinez-Lacaci, N. Kim, B. Wallace-Jones, M. E. Lippman, A. D. Ebert, C. Wechselberger, and D. S. Salomon.** 1999. Cripto-1 indirectly stimulates the tyrosine phosphorylation of erb B-4 through a novel receptor. J. Biol. Chem. **274:**8624–8629.
5. **Bianco, C., L. Strizzi, A. Rehman, N. Normanno, C. Wechselberger, Y. Sun, N. Khan, M. Hirota, H. Adkins, K. Williams, R. U. Margolis, M. Sanicola, and D. S. Salomon.** 2003. A Nodal- and ALK4-independent signaling pathway activated by Cripto-1 through glypican-1 and c-Src. Cancer Res. **63:** 1192–1197.
6. **Chen, X., D. Zhang, G. Dennert, G. Hung, and A. S. Lee.** 2000. Eradication of murine mammary adenocarcinoma through HSVtk expression directed by the glucose-starvation inducible grp78 promoter. Breast Cancer Res. Treat. **59:**81–90.
7. **Davidson, D. J., C. Haskell, S. Majest, A. Kherzai, D. A. Egan, K. A. Walter, A. Schneider, E. F. Gubbins, L. Solomon, Z. Chen, R. Lesniewski, and J. Henkin.** 2005. Kringle 5 of human plasminogen induces apoptosis of endothelial and tumor cells through surface-expressed glucose-regulated protein 78. Cancer Res. **65:**4663–4672.
8. **Delpino, A., and M. Castelli.** 2002. The 78 kDa glucose-regulated protein (GRP78/BIP) is expressed on the cell membrane, is released into cell culture medium and is also present in human peripheral circulation. Biosci. Rep. **22:**407–420.
9. **Delpino, A., P. Piselli, D. Vismara, S. Vendetti, and V. Colizzi.** 1998. Cell surface localization of the 78 kD glucose regulated protein (GRP 78) induced by thapsigargin. Mol. Membr. Biol. **15:**21–26.
10. **Dong, D., L. Dubeau, J. Bading, K. Nguyen, M. Luna, H. Yu, G. Gazit-Bornstein, E. M. Gordon, C. Gomer, F. L. Hall, S. S. Gambhir, and A. S. Lee.** 2004. Spontaneous and controllable activation of suicide gene expression driven by the stress-inducible grp78 promoter resulting in eradication of sizable human tumors. Hum. Gene Ther. **15:**553–561.
11. **Gazit, G., G. Hung, X. Chen, W. F. Anderson, and A. S. Lee.** 1999. Use of the glucose starvation-inducible glucose-regulated protein 78 promoter in suicide gene therapy of murine fibrosarcoma. Cancer Res. **59:**3100–3106.
12. **Gray, P. C., C. A. Harrison, and W. Vale.** 2003. Cripto forms a complex with activin and type II activin receptors and can block activin signaling. Proc. Natl. Acad. Sci. USA **100:**5193–5198.
13. **Gray, P. C., G. Shani, K. Aung, J. Kelber, and W. Vale.** 2006. Cripto binds transforming growth factor β (TGF-β) and inhibits TGF-β signaling. Mol. Cell. Biol. **26:**9268–9278.
14. **Harrison, C. A., P. C. Gray, W. H. Fischer, C. Donaldson, S. Choe, and W. Vale.** 2004. An activin mutant with disrupted ALK4 binding blocks signaling via type II receptors. J. Biol. Chem. **279:**28036–28044.
15. **Jamora, C., G. Dennert, and A. S. Lee.** 1996. Inhibition of tumor progression by suppression of stress protein GRP78/BiP induction in fibrosarcoma B/C10ME. Proc. Natl. Acad. Sci. USA **93:**7690–7694.
16. **Kinoshita, N., J. Minshull, and M. W. Kirschner.** 1995. The identification of two novel ligands of the FGF receptor by a yeast screening method and their activity in Xenopus development. Cell **83:**621–630.
17. **Lee, A. S.** 2005. The ER chaperone and signaling regulator GRP78/BiP as a monitor of endoplasmic reticulum stress. Methods **35:**373–381.
18. **Lee, A. S.** 2001. The glucose-regulated proteins: stress induction and clinical applications. Trends Biochem. Sci. **26:**504–510.
19. **Lee, A. S.** 2007. GRP78 induction in cancer: therapeutic and prognostic implications. Cancer Res. **67:**3496–3499.
20. **Mintz, P. J., J. Kim, K. A. Do, X. Wang, R. G. Zinner, M. Cristofanilli, M. A. Arap, W. K. Hong, P. Troncoso, C. J. Logothetis, R. Pasqualini, and W. Arap.** 2003. Fingerprinting the circulating repertoire of antibodies from cancer patients. Nat. Biotechnol. **21:**57–63.
21. **Misra, U. K., R. Deedwania, and S. V. Pizzo.** 2006. Activation and cross-talk between Akt, NF-kappaB, and unfolded protein response signaling in 1-LN prostate cancer cells consequent to ligation of cell surface-associated GRP78. J. Biol. Chem. **281:**13694–13707.
22. **Misra, U. K., R. Deedwania, and S. V. Pizzo.** 2005. Binding of activated alpha2-macroglobulin to its cell surface receptor GRP78 in 1-LN prostate cancer cells regulates PAK-2-dependent activation of LIMK. J. Biol. Chem. **280:**26278–26286.
23. **Misra, U. K., M. Gonzalez-Gronow, G. Gawdi, J. P. Hart, C. E. Johnson, and S. V. Pizzo.** 2002. The role of Grp 78 in alpha 2-macroglobulin-induced signal transduction. Evidence from RNA interference that the low density lipoprotein receptor-related protein is associated with, but not necessary for, GRP 78-mediated signal transduction. J. Biol. Chem. **277:**42082–42087.
24. **Misra, U. K., M. Gonzalez-Gronow, G. Gawdi, F. Wang, and S. V. Pizzo.** 2004. A novel receptor function for the heat shock protein Grp78: silencing of Grp78 gene expression attenuates alpha2M*-induced signalling. Cell. Signal. **16:**929–938.
25. **Mitra, S. K., and D. D. Schlaepfer.** 2006. Integrin-regulated FAK-Src signaling in normal and cancer cells. Curr. Opin. Cell Biol. **18:**516–523.
26. **Miyoshi, H., U. Blomer, M. Takahashi, F. H. Gage, and I. M. Verma.** 1998. Development of a self-inactivating lentivirus vector. J. Virol. **72:**8150–8157.
27. **Pardali, K., and A. Moustakas.** 2007. Actions of TGF-beta as tumor suppressor and pro-metastatic factor in human cancer. Biochim. Biophys. Acta **1775:**21–62.
28. **Reddy, R. K., C. Mao, P. Baumeister, R. C. Austin, R. J. Kaufman, and A. S. Lee.** 2003. Endoplasmic reticulum chaperone protein GRP78 protects cells from apoptosis induced by topoisomerase inhibitors: role of ATP binding site in suppression of caspase-7 activation. J. Biol. Chem. **278:**20915–20924.
29. **Schier, A. F.** 2003. Nodal signaling in vertebrate development. Annu. Rev. Cell Dev. Biol. **19:**589–621.
30. **Shen, M. M., and A. F. Schier.** 2000. The EGF-CFC gene family in vertebrate development. Trends Genet. **16:**303–309.
31. **Shin, B. K., H. Wang, A. M. Yim, F. Le Naour, F. Brichory, J. H. Jang, R. Zhao, E. Puravs, J. Tra, C. W. Michael, D. E. Misek, and S. M. Hanash.** 2003. Global profiling of the cell surface proteome of cancer cells uncovers an abundance of proteins with chaperone function. J. Biol. Chem. **278:**7607–7616.
32. **Siegel, P. M., and J. Massague.** 2003. Cytostatic and apoptotic actions of TGF-beta in homeostasis and cancer. Nat. Rev. Cancer **3:**807–821.
33. **Singer, O., R. A. Marr, E. Rockenstein, L. Crews, N. G. Coufal, F. H. Gage, I. M. Verma, and E. Masliah.** 2005. Targeting BACE1 with siRNAs ameliorates Alzheimer disease neuropathology in a transgenic model. Nat. Neurosci. **8:**1343–1349.
34. **Strizzi, L., C. Bianco, N. Normanno, and D. Salomon.** 2005. Cripto-1: a multifunctional modulator during embryogenesis and oncogenesis. Oncogene **24:**5731–5741.
35. **Topczewska, J. M., L. M. Postovit, N. V. Margaryan, A. Sam, A. R. Hess, W. W. Wheaton, B. J. Nickoloff, J. Topczewski, and M. J. Hendrix.** 2006. Embryonic and tumorigenic pathways converge via Nodal signaling: role in melanoma aggressiveness. Nat. Med. **12:**925–932.
36. **Triantafilou, K., D. Fradelizi, K. Wilson, and M. Triantafilou.** 2002. GRP78, a coreceptor for coxsackievirus A9, interacts with major histocompatibility complex class I molecules which mediate virus internalization. J. Virol. **76:**633–643.
37. **Triantafilou, K., and M. Triantafilou.** 2003. Lipid raft microdomains: key sites for Coxsackievirus A9 infectious cycle. Virology **317:**128–135.
38. **Watanabe, K., C. Bianco, L. Strizzi, S. Hamada, M. Mancino, V. Bailly, W. Mo, D. Wen, K. Miatkowski, M. Gonzales, M. Sanicola, M. Seno, and D. S. Salomon.** 2007. Growth factor induction of cripto-1 shedding by GPI-phospholipase D and enhancement of endothelial cell migration. J. Biol. Chem.
39. **Wilding, G., G. Zugmeier, C. Knabbe, K. Flanders, and E. Gelmann.** 1989. Differential effects of transforming growth factor beta on human prostate cancer cells in vitro. Mol. Cell. Endocrinol. **62:**79–87.
40. **Yeo, C., and M. Whitman.** 2001. Nodal signals to Smads through Cripto-dependent and Cripto-independent mechanisms. Mol. Cell **7:**949–957.